scientific reports



OPEN

KIAA1429 promotes non-smallcell lung cancer cell proliferation through the TRERNA1/HOXA6 axis

Yunxia Li^{1⊠}, Shiyao Tian¹ & Biao Yang^{2⊠}

Non-small-cell lung cancer (NSCLC) is the most common type of lung cancer. This study aimed to investigate the mechanism of vir-like m6A methyltransferase-associated protein (VIRMA, also called KIAA1429) in NSCLC cell proliferation. Levels of KIAA1429, long-chain non-coding RNAs translation regulatory long non-coding RNA 1 (IncRNATRERNA1), and homeobox A6 (HOXA6) were measured in NSCLC cells and normal cells. The enrichment of KIAA1429 and m6A on IncRNA TRERNA1 was detected. LncRNA TRERNA1 stability and subcellular localization of lncRNA TRERNA1 were detected. The binding of EZH2 to IncRNA TRERNA1 was analyzed. The enrichment of EZH2 and H3K27me3 on the HOXA6 promoter was analyzed. The mechanism of KIAA1429 was validated in vivo. KIAA1429 and IncRNA TRERNA1 were overexpressed in NSCLC cells and HOXA6 was downregulated. Knockdown of KIAA1429 significantly reduced NSCLC cell proliferation. KIAA1429 enhanced IncRNA TRERNA1 RNA stability via m6A modification and upregulated IncRNA TRERNA1 expression, which recruited EZH2 and increased H3K27me3 modification in the HOXA6 promoter region, thus suppressing HOXA6 expression. LncRNATRERNA1 overexpression or HOXA6 downregulation alleviated the inhibitory effect of KIAA1429 downregulation on NSCLC cell proliferation. KIAA1429 downregulation inhibited NSCLC cell proliferation in vivo. In conclusion, KIAA1429 promotes NSCLC proliferation through the TRERNA1/HOXA6 axis.

Keywords KIAA1429, NSCLC, TRERNA1, HOXA6, Cell proliferation

Lung cancer (LC) stands as the preeminent contributor to cancer-related deaths globally, with non-small cell lung cancer (NSCLC) being the predominant type (85%) and coughing, hemoptysis, dyspepsia, and chest pain as common symptoms¹. LC is considered an age-related disease, and other significant risk factors include a history of smoking, passive inhalation of secondhand smoke, and exposure to cooking fumes². Despite the demonstrated efficacy of chemotherapeutic agents including crizotinib, alectinib, and ceritinib, drug resistance and metastasis continue to pose considerable hurdles in the management of NSCLC³. Targeted therapy is an emerging and promising approach that has improved the treatment outcomes of NSCLC to a certain extent⁴. Therefore, studying the molecular targets for NSCLC is crucial for the treatment of NSCLC.

N6-methyladenosine (m6A) is the most prevalent RNA modification in eukaryotic cells, which can be added, removed, or recognized by m6A "writers," "erasers," and "readers" to modulate crucial biological processes⁵. Virlike m6A methyltransferase associated (KIAA1429), part of the m6A methyltransferase complex, orchestrates the regulation of downstream target genes by facilitating the recruitment of the catalytic core to introduce m6A modifications, thereby exerting a tumorigenic role in tumor growth⁶. Prior investigations have unveiled the tumorigenic functions of KIAA1429 across diverse cancer types. For example, KIAA1429 is upregulated in hepatocellular carcinoma tissues and promotes lung metastasis and tumor progression⁷. KIAA1429 elevates BTG2 expression in an m6A-dependent manner, consequently amplifying the proliferative and migratory capacities of lung adenocarcinoma cells⁸. KIAA1429 promotes NSCLC cell proliferation, migration, and resistance to gefitinib⁹. Our study further explored the role of KIAA1429 in NSCLC through m6A modification.

Long non-coding RNAs (lncRNAs) are RNA transcripts of more than 200 nucleotides in length that do not encode proteins and are involved in cell cycle, differentiation, and metabolic processes¹⁰. The transcriptional regulation of lncRNAs can be mediated through m6A modifications facilitated by the enzymatic activity of KIAA1429¹¹. Of note, lncRNA TRERNA1 is a newly discovered lncRNA that is aberrantly expressed in various cancers, including hepatocellular carcinoma, gastric cancer, and colorectal cancer^{11–13}. Interestingly, the

¹Department of Respiratory and Critical Care Medicine, Shenyang Fourth People's Hospital, No. 20 Huanghe South Street, Huanggu District, Shenyang City 110082, Liaoning Province, China. ²Department of Pathogenic Biology, School of Basic Medicine, Shenyang Medical College, No. 146 Huanghe North Street, Huanggu District, Shenyang City 110034, Liaoning Province, China. [△]email: 782186096@qq.com; yangbiao1125@symc.edu.cn

tumorigenic function of lncRNA TRERNA1 in NSCLC has been substantiated ¹⁴and lncRNA TRERNA1 may be regulated by m6A modification and thus participate in cancer progression ¹⁵. Additionally, lncRNAs can regulate downstream genes involved in NSCLC by interacting with RNA-binding proteins, such as enhancer of zeste homolog 2 (EZH2), suppressor of zeste 12 (SUZ12), and lysine-specific demethylase 1 (LSD1) ¹⁶. In this study, we proposed a novel downstream mechanism of lncRNA TRERNA1 through RNA-binding proteins in NSCLC.

The homeobox (HOX) genes, encoding a conserved family of transcription factors characterized by the presence of the homeodomain, are pivotal in the development and advancement of malignancies¹⁷. HOXA6, as a member of the HOX family, is significantly downregulated in NSCLC¹⁸. Moreover, HOXA6 expression is modulated by lncRNAs in cancer progression¹⁹. Nevertheless, the specific pathways and mechanisms of HOXA6 in NSCLC are still under investigation.

This study first focuses on elucidating the mechanism of KIAA1429 in regulating the expression of lncRNA TRERNA1 through m6A modification and thus controls the proliferation of NSCLC cells, providing a new theoretical basis for the treatment of NSCLC.

Materials and methods

Ethics statement

The animal experiment was approved by the ethics committee of Shenyang Fourth People's Hospital. All procedures for the use, care, and handling of animals were in accordance with the Guide for the Care and Use of Laboratory Animals by the National Institutes of Health²⁰. All methods are reported in accordance with ARRIVE guidelines for the reporting of animal experiments.

Cell culture

Human normal lung epithelial cell line (BEAS-2B) and human NSCLC cell lines (H1573, A549, SK-MES-1 and H520) were procured from the American Type Culture Collection (Manassas, VA, USA) and were cultured in Dulbecco's modified Eagle medium (DMEM) containing 10% fetal bovine serum (FBS, Sigma-Aldrich, St. Louis, MO, USA) at 37 °C with 5% CO₃.

Cell treatment

Three small interfering RNAs (siRNAs) targeting KIAA1429 (si-KIAA1429#1, si-KIAA1429#2, and si-KIAA1429#3), HOXA6 siRNAs (si-HOXA6 #1, si-HOXA6 #2, and si-HOXA6 #3), EZH2 siRNA (si-EHZ2), and negative control (si-NC), as well as the TRERNA1 overexpression vector (oe-TRERNA1) and a negative control empty vector (oe-NC), were purchased from RiboBio (Guangzhou, Guangdong, China). Upon reaching 80% confluency, cells were transfected using Lipofectamine 2000 (Invitrogen, Carlsbad, CA, USA).

Cell counting kit-8 (CCK-8) method

Transfected cells were assessed for relative cell viability at 24-, 48-, and 72-hours post-transfection using the CCK-8 (Bimake, Shanghai, China) according to the manufacturer's instructions. In brief, 5×10^3 cells were cultured in 96-well plates at 37 °C. Subsequently, each well was supplemented by 10 μ L of CCK-8 solution, followed by a 1-hour incubation at 37 °C. The optical density at 450 nm was measured using an HM-SY96S microplate reader (Hengmei Intelligent Manufacturing, Weifang, Shandong, China).

Colony formation assay

In the colony formation assay, 500 cells were seeded in 6-well plates and cultured for 2 weeks in a humidified atmosphere at 37 °C with 5% CO₂. The cell colonies were washed with phosphate buffer solution (PBS), fixed with 4% paraformaldehyde, and stained with 0.1% crystal violet (1 mg/mL) for 20 min. Subsequently, the cell colonies were imaged using a BX51 microscope (Olympus, Tokyo, Japan).

5-Ethynyl-2'-deoxyuridine (EdU) staining assay

Cell proliferation was assessed using the EdU detection kit (RiboBio) according to the manufacturer's instructions. Cells were cultured in 96-well plates (5×10^3 cells/well) and incubated for 2 h at 37 °C with 5% CO $_2$, with EdU labeling medium (10 μ L) added to each well. After treatment with 4% paraformaldehyde and 0.5% Triton X-100, cells were stained with anti-EdU working solution and Hoechst 33,342. Subsequently, cells were observed utilizing a fluorescence microscope (Olympus). The EdU incorporation rate was calculated as the ratio of EdU-positive cells to the total number of Hoechst 33,342-positive cells.

m6A quantitative analysis

Following the manufacturer's protocol, the m6A RNA methylation detection kit (ab185912, Abcam, Cambridge, MA, USA) was used to measure the total m6A levels in extracted RNA samples. The m6A percentage was determined by total RNA sample in each group. Absorbance at 450 nm was measured using a microplate reader, and the percentage of m6A in total RNA was calculated.

Actinomycin D treatment

Transcription inhibitor actinomycin D (Sigma-Aldrich) was used to analyze the stability of TRERNA1 RNA. Cells were seeded in 6-well plates and treated with 5 μ g/mL actinomycin D for 0, 3, and 6 h, and then lysed using TRIzol reagent (Invitrogen). RNA levels were analyzed by reverse transcription quantitative polymerase chain reaction (RT-qPCR).

Nuclear-cytoplasmic fractionation assay

Cellular localization was conducted using the PARIS kit (Invitrogen) according to the manufacturer's instructions. In brief, cellular nuclear and cytoplasmic fractions were separated, followed by RT-qPCR analysis. U6 snRNA and glyceraldehyde-3-phosphate dehydrogenase (GAPDH) were used as positive controls for nuclear and cytoplasmic fractions, respectively.

RNA Immunoprecipitation (RIP) assay

RIP assay was executed employing the Magna RIP[™] kit or Magna MeRIP[™] m6A kit (Millipore, Billerica, MA, USA). The antibodies against m6A (ab208577, Abcam), EZH2 (ab191250, Abcam), LSD1 (ab129195, Abcam), SUZ12 (ab175187, Abcam), and Ago2 (ab186733, Abcam) were used to prepare the immunoprecipitated protein-RNA complexes. Briefly, cells were fixed with 1% formaldehyde for 20 min and then resuspended in RIP lysis buffer. The cell lysates were incubated with a negative control immunoglobulin G (IgG, ab170190/ab172730, Abcam) or target antibodies at 4 °C overnight to prepare the immunoprecipitated protein-RNA complexes. Protein A/G magnetic beads were then added to the cell lysates, followed by washing with RIP wash buffer. Subsequently, RNA was extracted from the immunoprecipitated protein-RNA complexes for PCR analysis.

Chromatin Immunoprecipitation (ChIP)

ChIP assays were executed employing the EZ ChIP[™] kit (Millipore) following the manufacturer's instructions. Briefly, cross-linked chromatin DNA was sonicated into fragments, followed by fixation with 1% formaldehyde. Immunoprecipitation was carried out using antibodies against EZH2 (ab191250, Abcam), H3K27me3 (ab192985, Abcam), and normal mouse IgG (negative control; ab172730, Abcam). DNA was then extracted for PCR analysis (Table 1).

Xenograft tumor assay in nude mice

BALB/c nude mice (6–8 weeks old, 18–20 g, male) were purchased from SJA Experimental Animal Co., Ltd (Changsha, Hunan, China). The mice were maintained under a 12-hour light-dark cycle at 18–23 °C and a humidity of 40–60%. A549 cells were infected with lentivirus carrying short hairpin RNA targeting KIAA1429 (sh-KIAA1429) or negative control (sh-NC) and resuspended in PBS. Subsequently, 5×10^6 cells in 200 μ L PBS were subcutaneously injected into the flank of each mouse. Tumor length and width were measured with calipers on the anterior flank of each mouse every 3 days, and the calculation of tumor volume was conducted as the formula V=length \times width² /2. After 21 days, the mice were euthanized by intraperitoneal injection of 200 mg/kg pentobarbital sodium, and the weight of the xenograft tumors was measured.

Immunohistochemistry

For immunohistochemical staining, tissue sections were deparaffinized and rehydrated. The sections were then incubated overnight at 4 °C with antibodies against Ki-67 (ab16667, Abcam) and PCNA (ab92552, Abcam). Subsequently, target proteins were detected using 3,3'-Diaminobenzidine (DAB) staining solution (ZSGB-BIO, Beijing, China) according to the manufacturer's instructions.

RT-qPCR

Extraction of total RNA was conducted using TRIzol reagent (Invitrogen), and complementary DNA (cDNA) was synthesized using a reverse transcription kit (Accurate Biology, Changsha, Hunan, China). RT-qPCR was carried out employing SYBR Green Master Mix (Accurate Biology) and the Applied Biosystems 7500 Real-time PCR system (Thermo Fisher Scientific, Waltham, MA, USA). Following the reaction, the relative gene expression levels were calculated using the $2^{-\Delta\Delta Ct}$ method²¹. The PCR primers are listed in Table 1, with GAPDH as the reference gene.

Western blot assay

Cells were washed with PBS and lysed in radioimmunoprecipitation (RIPA) buffer (Beyotime, Shanghai, China). To remove any cell debris, cells were lysed on ice, and the lysates were centrifuged at 12,000 g for 30 min at 4 °C. Proteins were separated by sodium dodecyl sulfate-polyacrylamide gel electrophoresis and transferred onto

Gene	Sequences (5'-3')
HOXA6	F: TTCCACTTCAACCGCTACCT
	R: TGGGCTGCGTGGAATTGATG
TRERNA1	F: CTGGAAATCCTCCACCTCGG
	R: AGGACTGGCTGAGGTTTGTG
KIAA1429	F: CGAGCGCTGAGCAAAGTTCT
	R: TGGGGGTATGACTCGGACTT
HOXA6 promoter	F: TAAGGCGCACGAGTGAAGAG
	R: ATTCGTGGGTGCGAGTTCTT
GAPDH	F: GATGCTGGCGCTGAGTACG
	R: GCTAAGCAGTTGGTGGTGC

Table 1. PCR primer sequences.

polyvinylidene fluoride membranes (Bio-Rad Laboratories, Hercules, CA, USA). The membranes were blocked in 5% non-fat milk, followed by overnight incubation at 4 °C with primary antibodies against HOXA6 (PA5-97836, 1:1000, Thermo Fisher Scientific), KIAA1429 (ab271136, 1:1000, Abcam), EZH2 (ab191250, 1:1000, Abcam), and β-actin (ab8227, 1:1000, Abcam). After three times of washing, the membranes were incubated with a secondary antibody (ab205718, 1:2000, Abcam) at room temperature for 2 h. Protein bands were visualized using Western Lightning Plus-ECL (PerkinElmer, Waltham, MA, USA), and the gray value was quantified using ImageJ 1.52v. Original blots/gels are presented in Supplementary Fig. 1.

Statistical analysis

SPSS 21.0 (IBM, Armonk, NY, USA) and GraphPad Prism 8.0 software (GraphPad Software Inc., San Diego, CA, USA) were used for statistical analysis and data plotting. First, normality and homogeneity of variance tests were conducted, which verified that the data were in normal distribution and homogeneity of variance. Data comparison between two groups was performed using t-test. Data comparisons among multiple groups were performed using one-way or two-way analysis of variance (ANOVA), followed by Tukey's multiple comparisons test for post hoc analysis. p value was obtained via two-sided tests; p < 0.05 indicated a statistically significant difference and p < 0.01 indicated a highly significant difference.

Results

KIAA1429 is highly expressed in NSCLC and promotes NSCLC cell proliferation

The expression of KIAA1429 in various cell lines was detected by RT-qPCR and Western blot assays, revealing high expression of KIAA1429 in NSCLC cell lines (p < 0.05, Fig. 1A-B). Subsequently, the A549 cell line with relatively high KIAA1429 expression and the H520 cell line with relatively low KIAA1429 expression were selected for further validation. Downregulation of KIAA1429 in A549 and H520 cells was achieved by transfection with si-KIAA1429, while si-KIAA1429#1 and si-KIAA1429#3 exhibiting good transfection efficiency were selected for further experiments (p < 0.05, Fig. 1C-D). The results showed that upon downregulation of KIAA1429, the proliferation of NSCLC cells was decreased, clone proliferation was reduced, and the EdU incorporation rate was decreased (p < 0.05, Fig. 1E-G).

KIAA1429 targets the m6A modification site of LncRNA TRERNA1 and enhances LncRNA TRERNA1 RNA stability

KIAA1429 targets the m6Å modification site of lncRNA, enhancing its RNA stability²². Quantitative analysis of m6A showed a significant decrease in the m6A level in cells after downregulation of KIAA1429 (p < 0.05, Fig. 2A). LncRNA TRERNA1 is regulated by m6A modification and is highly expressed in NSCLC^{14,15}. RIP results revealed a notable decline in m6A levels of TRERNA1 RNA after downregulation of KIAA1429 (p < 0.05, Fig. 2B). Following actinomycin D treatment, the half-life of TRERNA1 RNA in the si-KIAA1429 group was significantly shorter than that in the si-NC group (p < 0.05, Fig. 2C). Additionally, RT-qPCR results confirmed an increase in TRERNA1 expression in NSCLC cell lines (p < 0.05, Fig. 2D), but additional downregulation of KIAA1429 decreased TRERNA1 expression (p < 0.05, Fig. 2E). In summary, KIAA1429 targets the m6A modification site of lncRNA TRERNA1, enhancing lncRNA TRERNA1 RNA stability.

Overexpression of LncRNATRERNA1 alleviates the inhibitory effect of KIAA1429 downregulation on NSCLC cell proliferation

Subsequently, we conducted combined experiments in A549 cells. We successfully upregulated TRERNA1 expression in cells (p<0.05, Fig. 3A) and co-treated the cells with si-KIAA1429#1. Compared to pc-NC transfection, the proliferation of cells was significantly increased after pc-TRERNA1 transfection (p<0.05, Fig. 3B). Furthermore, upregulation of TRERNA1 promoted the clone proliferation and EdU incorporation rate of cells (p<0.05, Fig. 3C-D). These results indicated that overexpression of TRERNA1 alleviates the inhibitory effect of KIAA1429 downregulation on NSCLC cell proliferation.

LncRNATRERNA1 recruits EZH2 to increase H3K27me3 modification in the HOXA6 promoter, thereby inhibiting HOXA6 expression

Recent studies have shown that IncRNAs can bind to RNA-binding proteins such as EZH2, SUZ12, and LSD1 to regulate the expression of downstream targets 16,23. Nuclear-cytoplasmic fractionation results indicated that TRERNA1 is primarily localized in the nucleus of NSCLC cells (Fig. 4A). RIP results demonstrated that EZH2, SUZ12, and LSD1 can all pull down TRERNA1, with EZH2 showing the most significant enrichment (p < 0.05, Fig. 4B), indicating a specific interaction between TRERNA1 and EZH2. To further investigate the binding between TRERNA1 and EZH2, we detected the expression of EZH2 using RT-qPCR and Western blot assays. Compared to the pc-NC group, there was no significant change in the expression of EZH2 in the pc-TRERNA1 group (p > 0.05, Fig. 4C-D). HOXA6 is known to be downregulated in NSCLC¹⁸. Our results consistently confirmed the downregulation of HOXA6 in NSCLC cell lines (*p* < 0.05, Fig. 4E-F). Our observations indicated that the depletion of EZH2 was associated with the upregulation of HOXA6 at the mRNA and protein levels (p<0.05, Fig. 4C-D and G-H). Subsequent ChIP experiments found that EZH2 directly bound to the HOXA6 promoter and induced H3K27me3 expression (p < 0.05, Fig. 4I). Furthermore, the enrichment of EZH2 and H3K27me3 levels on the HOXA6 promoter was reduced after downregulation of KIAA1429 and increased after upregulation of TRERNA1 (p<0.05, Fig. 4I). Downregulation of KIAA1429 led to upregulation of HOXA6 expression, while upregulation of TRERNA1 led to downregulation of HOXA6 expression (*p* < 0.05, Fig. 4G-H). In summary, lncRNA TRERNA1 recruits EZH2 to increase H3K27me3 modification in the HOXA6 promoter region, thereby inhibiting HOXA6 expression.

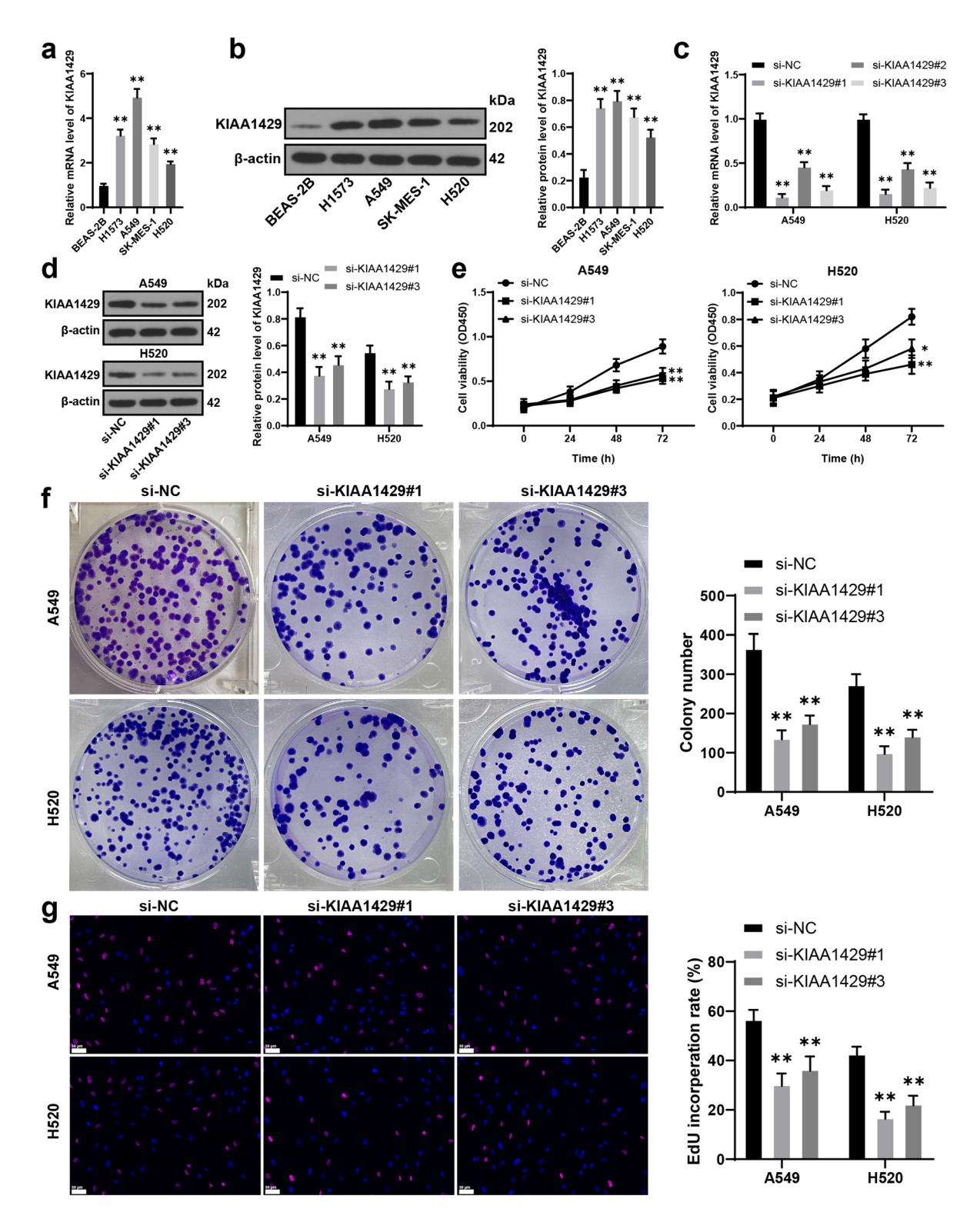


Fig. 1. KIAA1429 is highly expressed in NSCLC and promotes NSCLC cell proliferation. **A-B**: The expression of KIAA1429 in different cells was detected by RT-qPCR and Western blot. ** versus BEAS-2B, p < 0.01. **C-D**: The expression of KIAA1429 in different cells after transfection with siRNA was detected by RT-qPCR and Western blot. ** versus si-NC, p < 0.01. **E**: Cell proliferation was measured by CCK-8 assay. * versus si-NC, p < 0.05; ** versus si-NC, p < 0.01. **F**: Colony formation assay was performed to assess cell proliferation. ** versus si-NC, p < 0.01. **G**: EdU staining was used to measure the EdU incorporation rate. ** versus si-NC, p < 0.01. The experiments were independently repeated three times, and the data are presented as the mean \pm standard deviation. Data comparisons among multiple groups in panels A-B were analyzed by one-way ANOVA, and data comparisons among multiple groups in panels C-G were analyzed by two-way ANOVA, followed by Tukey's multiple comparisons test.

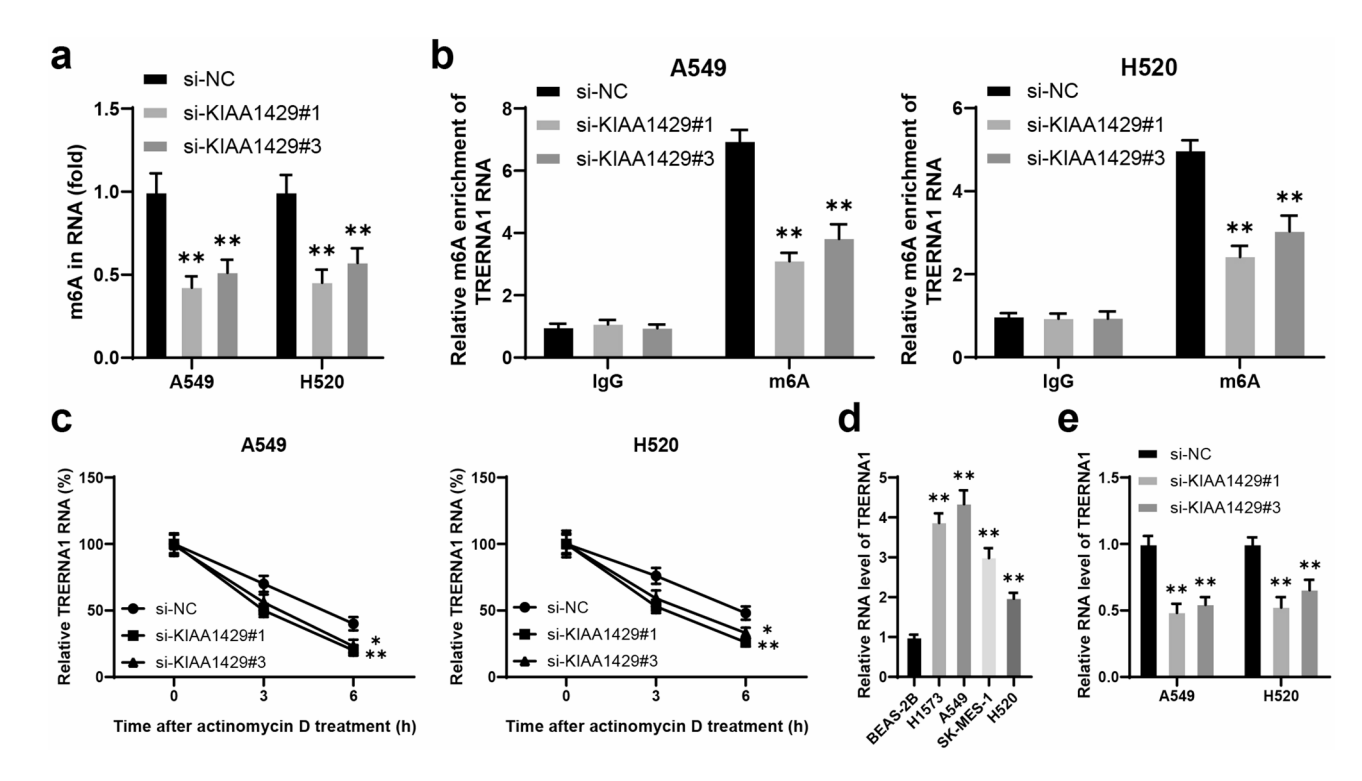


Fig. 2. KIAA1429 targets the m6A modification site of lncRNA TRERNA1 and enhances lncRNA TRERNA1 RNA stability. **A**: m6A quantitative analysis was performed to detect m6A levels in different cells after transfection with siRNA. ** versus si-NC, p < 0.01. **B**: RIP was used to detect m6A enrichment on TRERNA1 RNA. ** versus si-NC, p < 0.01. **C**: Following actinomycin D treatment, RT-qPCR was used to measure the expression of TRERNA1 in different cells. * versus si-NC, p < 0.05; ** versus si-NC, p < 0.01. **D**: RT-qPCR was used to detect the expression of TRERNA1 in different cells. ** versus BEAS-2B, p < 0.01. **E**: RT-qPCR was used to detect the expression of TRERNA1 in different cells. ** versus si-NC, p < 0.01. The experiments were independently repeated three times, and the data are presented as the mean ± standard deviation. Data comparisons among multiple groups in panel D were analyzed by one-way ANOVA, and data comparisons among multiple groups in panels A-C, E were analyzed by two-way ANOVA, followed by Tukey's multiple comparisons test.

Downregulation of HOXA6 alleviates the inhibitory effect of KIAA1429 downregulation on NSCLC cell proliferation

Subsequently, we knocked down HOXA6 expression in A549 cells using si-HOXA6#2 and si-HOXA6#3 with better transfection efficiency, and co-treated A549 cells with si-KIAA1429#1 (p<0.05, Fig. 5A-B). Compared to the downregulation of KIAA1429 alone, the combined group showed increased proliferation, clone proliferation, and EdU incorporation rate (p<0.05, Fig. 5C-E), indicating that downregulation of HOXA6 alleviates the inhibitory effect of KIAA1429 downregulation on NSCLC cell proliferation.

Downregulation of KIAA1429 inhibits NSCLC cell proliferation in vivo

We established a xenograft tumor model using A549 cells with stable downregulation of KIAA1429 and observed a decrease in tumor volume and weight following KIAA1429 downregulation. The positive rates of proliferation markers Ki67 and PCNA were also reduced following KIAA1429 downregulation (p<0.05, Fig. 6A-C). Additionally, compared to the sh-NC group, the sh-KIAA1429 group exhibited decreased m6A levels in tumor tissues, reduced expression of KIAA1429 and TRERNA1, and increased HOXA6 expression (p<0.05, Fig. 6D-F). These results indicated that KIAA1429 promotes NSCLC cell proliferation in vivo through the TRERNA1/HOXA6 axis.

Discussion

In recent years, molecular targeted therapy has made significant contributions to the screening, diagnosis, treatment, and prognosis of NSCLC²⁴. Our study elucidated that KIAA1429 upregulated lncRNA TRERNA1 expression in an m6A-dependent manner, enhanced EZH2 recruitment, promoted H3K27me3 modification on the HOXA6 promoter, inhibited HOXA6 expression, and ultimately increased the proliferation of NSCLC cells (Fig. 7).

KIAA1429, as a "writer" of m6A, is an important factor in abnormal m6A modification. Previous studies have found that KIAA1429 is aberrantly expressed in various malignant tumors^{7,25,26}. In lung adenocarcinoma, KIAA1429 knockdown significantly reduces overall m6A levels and increases the expression of the tumor suppressor BTG2 in an m6A modification-dependent manner, thus inhibiting cancer cell proliferation and

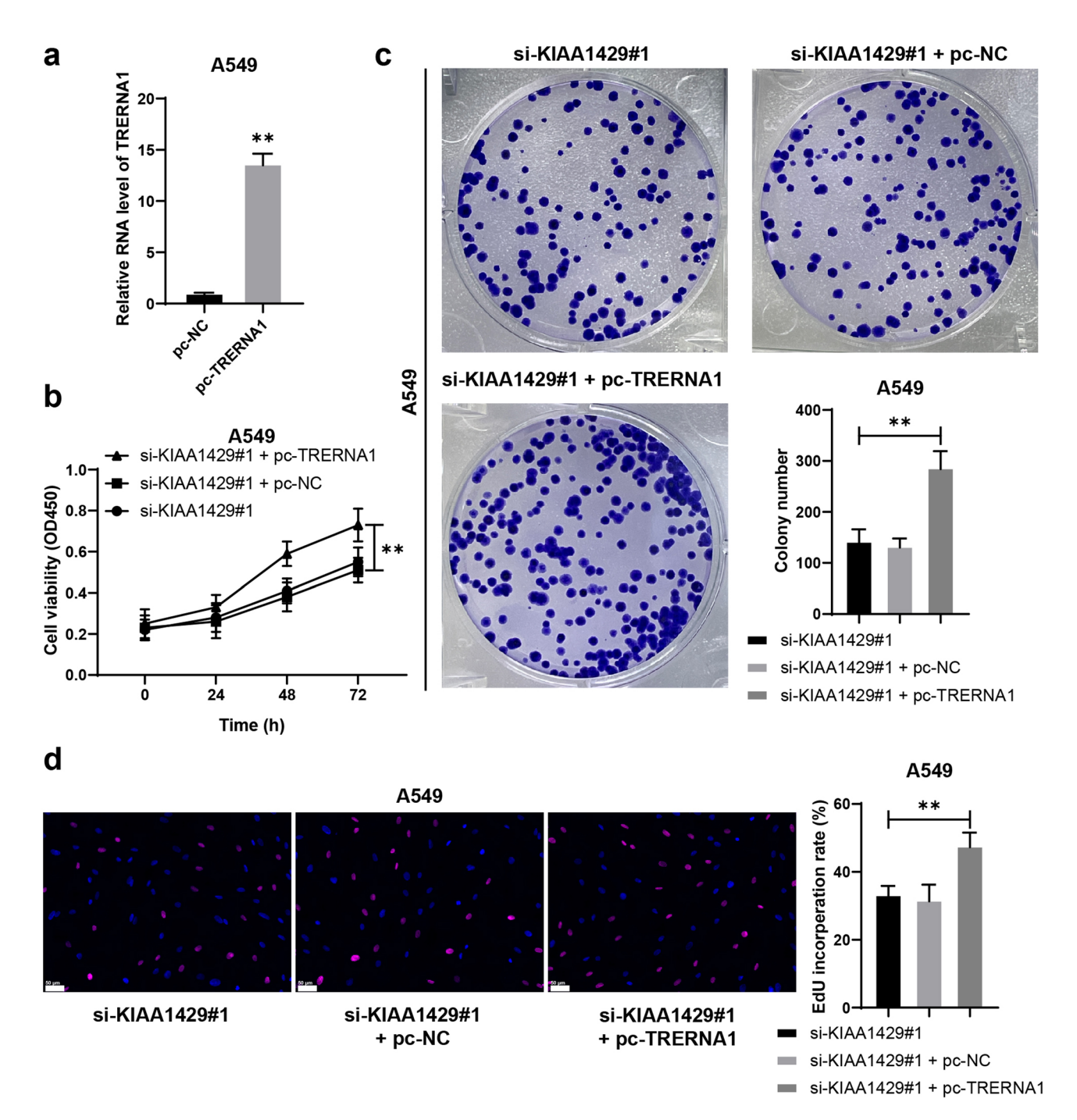
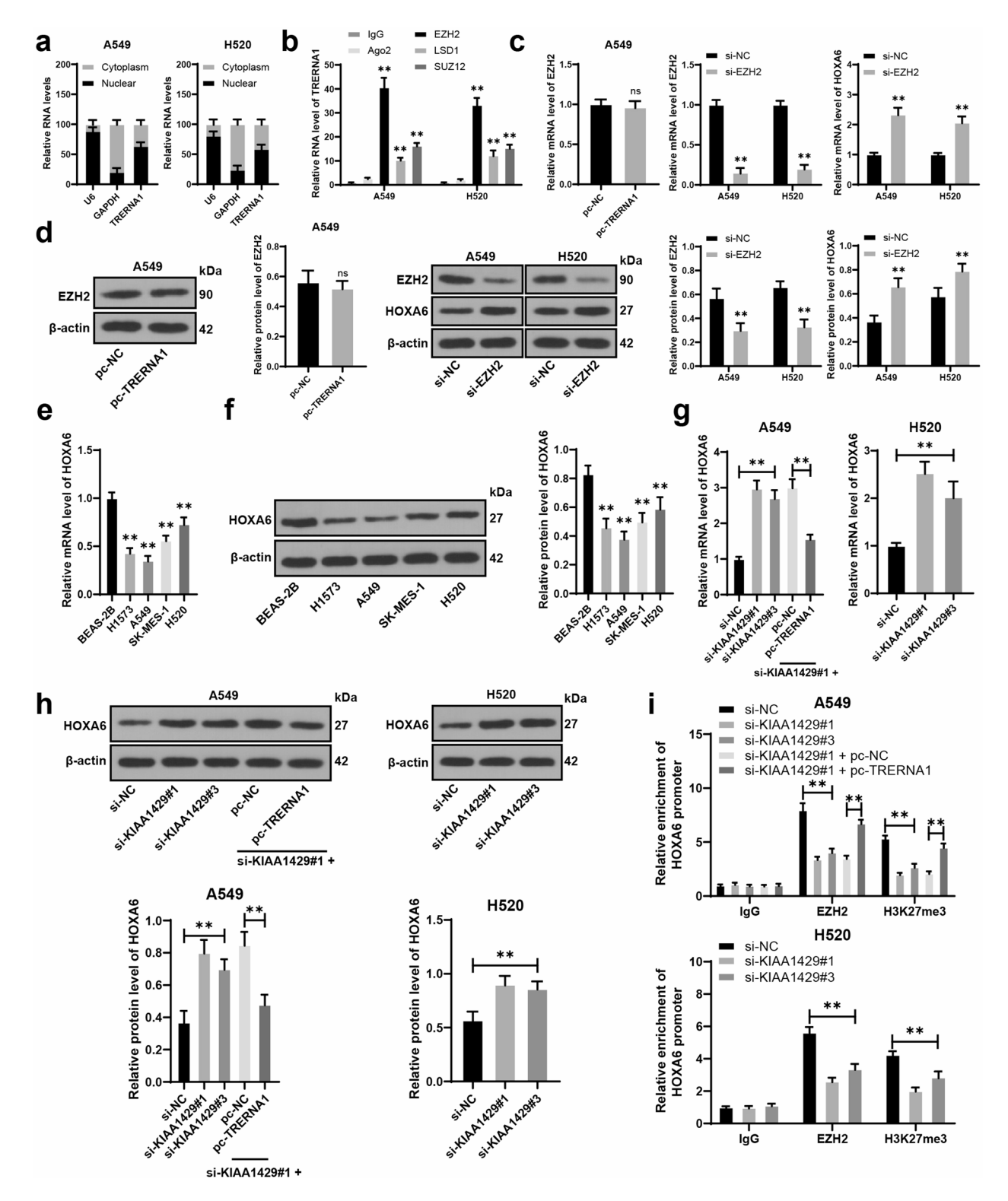


Fig. 3. Overexpression of lncRNA TRERNA1 alleviates the inhibitory effect of KIAA1429 downregulation on NSCLC cell proliferation. **A:** RT-qPCR was performed to detect the expression of TRERNA1 in A549 cells transfected with pc-NC or pc-TRERNA1. ** versus pc-NC, p < 0.01. **B:** Cell proliferation was measured using the CCK-8 assay. **C:** Colony formation assay was used to assess cell proliferation. **D:** EdU staining was performed to measure the EdU incorporation rate. The experiments were independently repeated three times, and the data are presented as the mean \pm standard deviation. Data comparisons between two groups in panel A were analyzed by t-test. Data comparisons among multiple groups in panels C-D were analyzed by one-way ANOVA, and data comparisons among multigroup in panel B were analyzed by two-way ANOVA, followed by Tukey's multiple comparisons test. ** t p < 0.01.

migration⁸. Notably, KIAA1429 is overexpressed in NSCLC, and downregulation of KIAA1429 results in decreased m6A modification levels, leading to reduced stability of HOXA1, thereby inhibiting tumor growth and cell migration⁹. In line with the above findings, our experimental data found that KIAA1429 was highly expressed in NSCLC cell lines. After downregulation of KIAA1429, the proliferation and clonogenicity of NSCLC cells were decreased. The in vivo experiments also proved the repressing effect of KIAA1429 silencing on



NSCLC cell proliferation. KIAA1429 enhances LINC01106 m6A modification to promote lung adenocarcinoma development²⁷. Our results indicated that downregulation of KIAA1429 reduced m6A levels and m6A modification of TRERNA1 in cells. Collectively, the oncogenic role of KIAA1429 is achieved by promoting m6A modification on lncRNA TRERNA1, increasing lncRNA TRERNA1 stability and expression.

In NSCLC patients, those with high expression of lncRNA TRERNA1 have a worse pathological stage and overall survival¹⁴. The overexpression of lncRNA TRERNA1 is associated with enhanced radioresistance in NSCLC cells²⁸. In this study, we consistently observed that the overexpression of lncRNA TRERNA1 promoted cell proliferation and colony formation. In addition, lncRNA TRERNA1 can recruit EZH2 in cancer cells, leading to the addition of H3K27me3 modification on the promoter regions of downstream target genes, thereby mediating their silencing^{11,15}. This pathway was further confirmed in our study. Superficially, lncRNA TRERNA1 interacted with EZH2. EZH2 mediates H3K27me3 expression to suppress downstream gene expression, thus

∢Fig. 4. LncRNA TRERNA1 recruits EZH2 to increase H3K27me3 modification in the HOXA6 promoter, thereby inhibiting HOXA6 expression. **A**: Nuclear-cytoplasmic separation assay was performed to detect the subcellular localization of TRERNA1. **B**: RIP analysis was conducted to assess the binding of TRERNA1 to RNA-binding proteins. ** versus IgG, *p* < 0.01. **C-D**: RT-qPCR and Western blot were used to detect the expression of EZH2 and HOXA6 in different cells. ns versus pc-NC, *p* > 0.05; ** versus si-NC, *p* < 0.01. **E-F**: RT-qPCR and Western blot were used to detect the expression of HOXA6 in different cells. ** versus BEAS-2B, *p* < 0.01. **G-H**: RT-qPCR and Western blot were used to detect the expression of HOXA6 in different cells. ** *p* < 0.01. **I**: ChIP was performed to assess the enrichment of EZH2 and H3K27me3 on the HOXA6 promoter. ** *p* < 0.01. The experiments were independently repeated three times, and the data are presented as the mean ± standard deviation. Data comparisons between two groups in panels C (left) and D (left) were analyzed by the *t*-test. Data comparisons among multiple groups in panels E-H were analyzed by one-way ANOVA, and data comparisons among multiple groups in panels B, C (middle, right), D (middle, right), and I were analyzed by two-way ANOVA, followed by Tukey's multiple comparisons test.

aggravating the progression of NSCLC²⁹. We observed that lncRNA TRERNA1 recruited EZH2, and EZH2 increased the enrichment of H3K27me3 on the HOXA6 promoter, resulting in the downregulation of HOXA6. Overall, lncRNA TRERNA1 promotes NSCLC tumorigenesis through the EZH2/H3K27me3/HOXA6 axis.

HOXA6 expression has been reported to be suppressed in breast cancer tissues³⁰ and clear cell renal cell carcinoma³¹. Our study also found downregulated HOXA6 in NSCLC cells and increased proliferation and colony numbers in NSCLC cells after further knocking down of HOXA6. Meanwhile, evidence suggests that HOXA6 expression increases in NSCLC cells following ionizing radiation and may potentially induce cell apoptosis and cell cycle arrest¹⁸. Another report has indicated that in clear cell renal cell carcinoma, overexpression of HOXA6 can inhibit the cell cycle at the G0/G1 phase, suppress proliferation, and promote levels of apoptotic factors³¹. In summary, si-HOXA6 promotes malignant proliferation in NSCLC. We hypothesized that overexpression of HOXA6 may exert anti-cancer effects in NSCLC by inducing cell apoptosis and inhibiting the cancer cell cycle, and further validation is necessary in future studies.

There are still some limitations in our study. Firstly, although the significance of KIAA1429 in NSCLC has been identified, the upstream mechanism of KIAA1429 remains unclear. Secondly, we only explored the role of a single mechanism in a limited cell line, and functional validation and interventions in normal lung cells were constrained by funding limitations. The effects of KIAA1429 on cell migration and apoptosis in NSCLC still need to be explored. Thirdly, due to logical and funding constraints, HOXA6 overexpression and EZH2 functional analysis were not performed, and small molecule inhibitors of KIAA1429 or antisense oligonucleotides targeting LncRNA TRERNA1 were not used for validation. Finally, the downstream mechanisms of HOXA6 require further investigation. In the future, we will explore the upstream mechanism of KIAA1429, introduce more cell lines to validate our results, investigate the role of KIAA1429 in cell migration, and elucidate the potential effects of the immune system on NSCLC, providing new theoretical knowledge for the treatment of NSCLC.

In conclusion, KIAA1429 targets the m6A modification site of lncRNA TRERNA1, enhancing the stability of lncRNA TRERNA1 and upregulating its expression. Overexpression of lncRNA TRERNA1 enhances the recruitment of EZH2, increases the H3K27me3 modification of the HOXA6 promoter, suppresses HOXA6 expression, and ultimately promotes the proliferation of NSCLC cells.

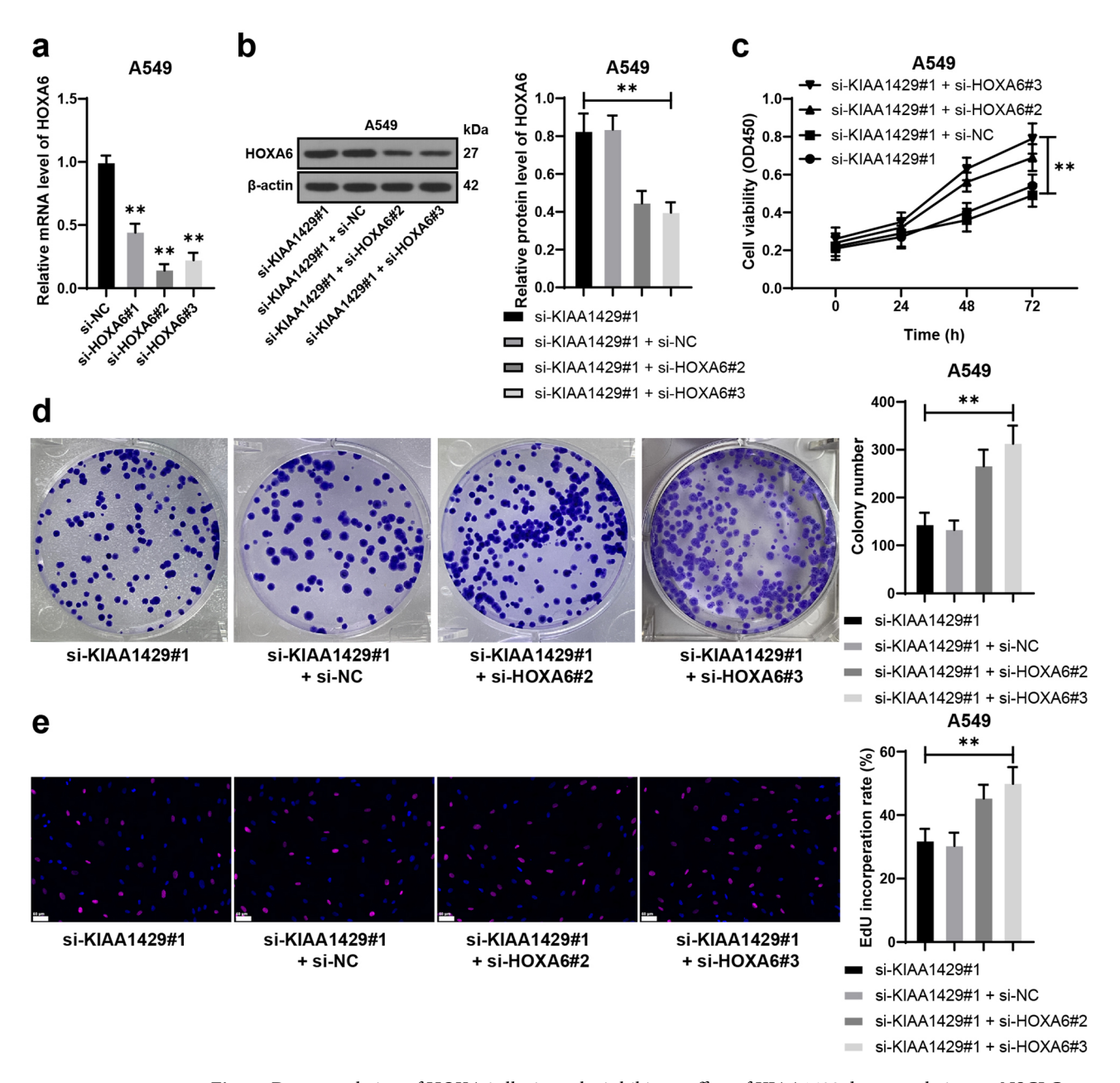


Fig. 5. Downregulation of HOXA6 alleviates the inhibitory effect of KIAA1429 downregulation on NSCLC cell proliferation. **A**: RT-qPCR was performed to detect the expression of HOXA6 in A549 cells transfected with si-NC or si-HOXA6. ** versus si-NC, p < 0.01. **B**: Western blot was used to detect the expression of HOXA6 in A549 cells. **C**: Cell proliferation was measured using the CCK-8 assay. **D**: Colony formation assay was used to assess cell proliferation. **E**: EdU staining was performed to measure the EdU incorporation rate. The experiments were independently repeated three times, and the data are presented as the mean \pm standard deviation. Data comparisons among multiple groups in panels A-B and D-E were analyzed by one-way ANOVA, and data comparisons among multiple groups in panel C were analyzed by two-way ANOVA, followed by Tukey's multiple comparisons test. ** p < 0.01.

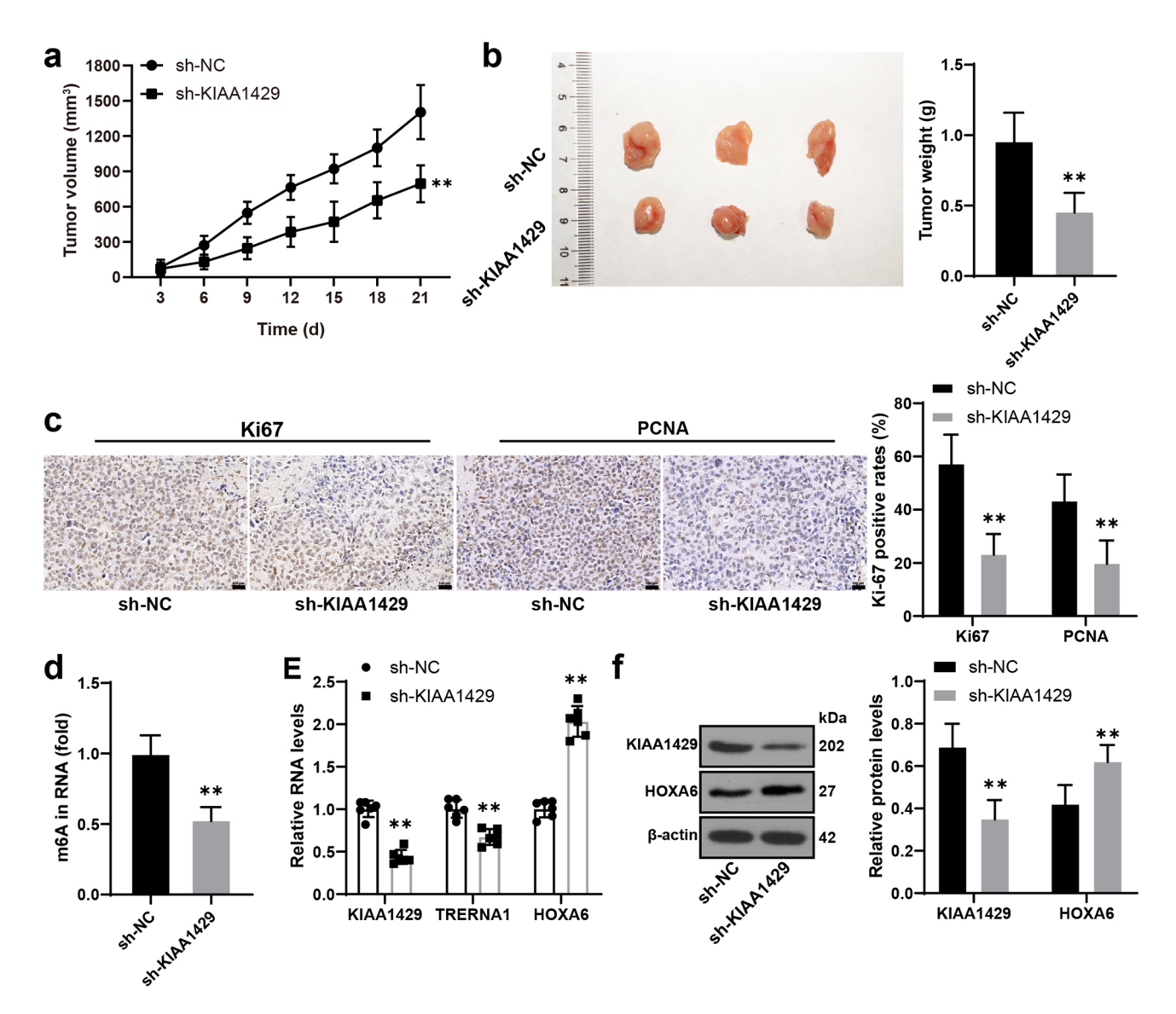


Fig. 6. Downregulation of KIAA1429 inhibits NSCLC cell proliferation in vivo. **A:** Tumor formation was induced by subcutaneous injection of A549 cells into nude mice. Tumor size was measured every 3 days, and the mice were euthanized on day 21, and tumor tissues were photographed. **B:** Tumor tissue weight and representative images. **C:** Immunohistochemistry was performed to detect the positive rates of Ki67 and PCNA in tumor tissues. **D:** m6A quantitative analysis was conducted to measure the m6A levels in the tissues. **E-F:** RT-qPCR and Western blot were used to detect the expression of KIAA1429, TRERNA1, and HOXA6 in tumor tissues. N=6, and the experiments were independently repeated three times. The data are presented as the mean \pm standard deviation. Data comparisons between two groups in panels B and D were analyzed by the t-test. Data comparisons among multiple groups in panels A, C, E, and F were analyzed by two-way ANOVA, followed by Tukey's multiple comparisons test. ** versus sh-NC, p < 0.01.

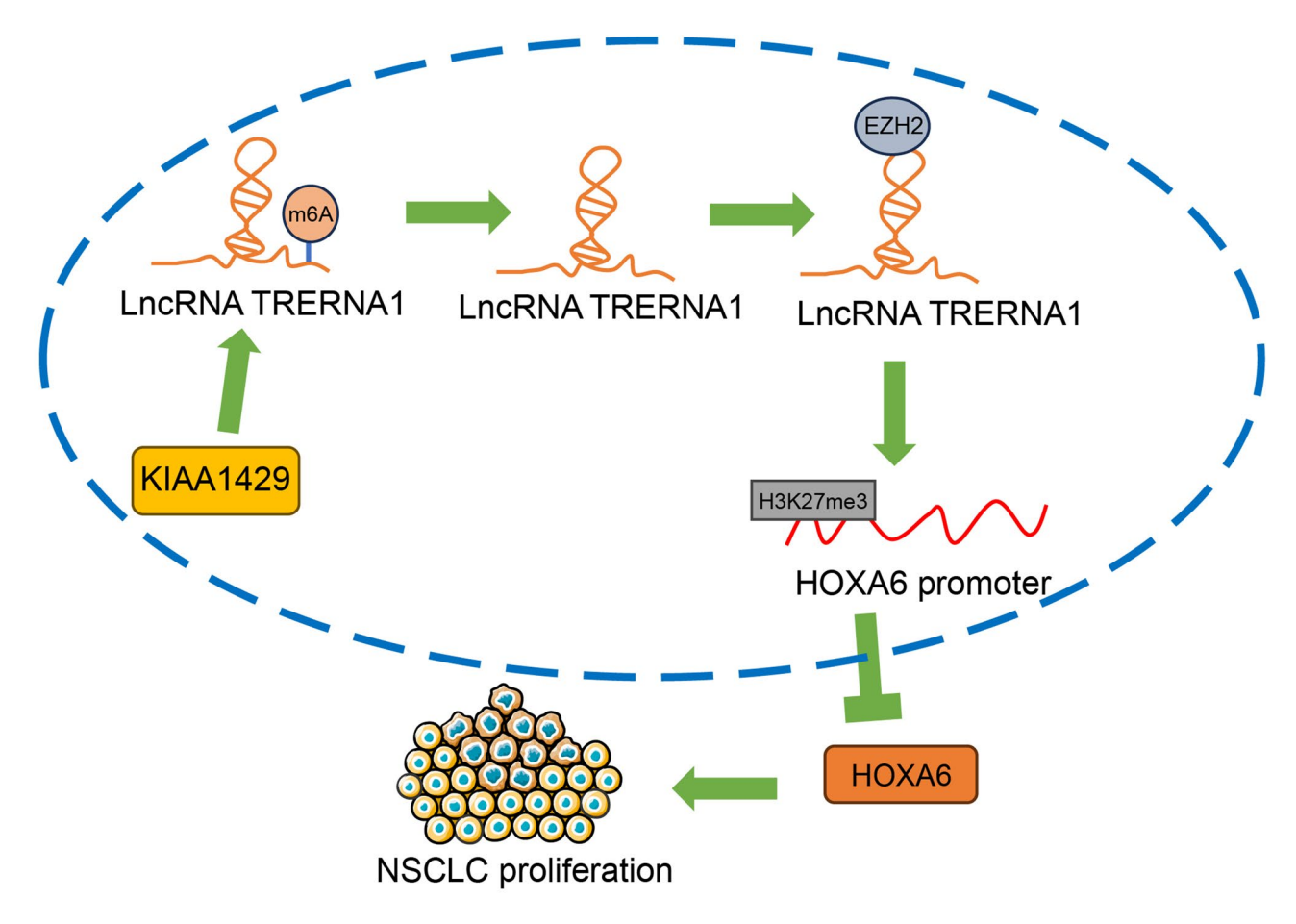


Fig. 7. Mechanism of KIAA1429-mediated m6A modification in promoting NSCLC cell proliferation. KIAA1429 targets m6A modification sites on the lncRNA TRERNA1, enhancing TRERNA1 RNA stability and upregulating the expression of TRERNA1, which in turn strengthens TRERNA1 recruitment of EZH2, leading to increased H3K27me3 modification in the HOXA6 promoter, thereby suppressing HOXA6 expression and promoting NSCLC cell proliferation.

Data availability

The datasets generated and/or analyzed during the current study are available from the corresponding author on reasonable request.

Received: 9 October 2024; Accepted: 27 June 2025

Published online: 10 July 2025

References

- Reck, M. & Rabe, K. F. Precision diagnosis and treatment for advanced Non-Small-Cell lung Cancer. N Engl. J. Med. 377, 849–861. https://doi.org/10.1056/NEJMra1703413 (2017).
- 2. Li, W. et al. Classic signaling pathways in alveolar injury and repair involved in Sepsis-Induced ALI/ARDS: new research progress and prospect. *Dis. Markers*. 6362344 https://doi.org/10.1155/2022/6362344 (2022). (2022).
- 3. Jonna, S. & Subramaniam, D. S. Molecular diagnostics and targeted therapies in non-small cell lung cancer (NSCLC): an update. *Discov Med.* 27, 167–170 (2019).
- 4. Liu, S. Y., Zhang, J. T., Zeng, K. H. & Wu, Y. L. Perioperative targeted therapy for oncogene-driven NSCLC. Lung Cancer. 172, 160–169. https://doi.org/10.1016/j.lungcan.2022.05.007 (2022).
- Sun, T., Wu, R. & Ming, L. The role of m6A RNA methylation in cancer. *Biomed. Pharmacother.* 112, 108613. https://doi.org/10.1 016/j.biopha.2019.108613 (2019).
- 6. He, R. et al. Itaconate inhibits ferroptosis of macrophage via Nrf2 pathways against sepsis-induced acute lung injury. *Cell. Death Discov.* 8, 43. https://doi.org/10.1038/s41420-021-00807-3 (2022).
- Lan, T. et al. KIAA1429 contributes to liver cancer progression through N6-methyladenosine-dependent post-transcriptional modification of GATA3. *Mol. Cancer.* 18, 186. https://doi.org/10.1186/s12943-019-1106-z (2019).
 Zhang, C. et al. Gene amplification-driven RNA methyltransferase KIAA1429 promotes tumorigenesis by regulating BTG2 via
- 8. Znang, C. et al. Gene amplification-driven KNA methyltransferase KIAA1429 promotes tumorigenesis by regulating B1G2 via m6A-YTHDF2-dependent in lung adenocarcinoma. *Cancer Commun. (Lond).* 42, 609–626. https://doi.org/10.1002/cac2.12325 (2022).
- 9. Tang, J., Han, T., Tong, W., Zhao, J. & Wang, W. N(6)-methyladenosine (m(6)A) methyltransferase KIAA1429 accelerates the gefitinib resistance of non-small-cell lung cancer. Cell. Death Discov. 7, 108. https://doi.org/10.1038/s41420-021-00488-y (2021).
- Bridges, M. C., Daulagala, A. C. & Kourtidis, A. LNCcation: LncRNA localization and function. J. Cell. Biol. 220 https://doi.org/1 0.1083/jcb.202009045 (2021).

- 11. Wu, H. et al. LncRNA TRERNA1 function as an enhancer of SNAI1 promotes gastric Cancer metastasis by regulating Epithelial-Mesenchymal transition. Mol. Ther. Nucleic Acids. 8, 291–299. https://doi.org/10.1016/j.omtn.2017.06.021 (2017).
- 12. Wang, W., Tang, X., Qu, H. & He, Q. Translation regulatory long non-coding RNA 1 represents a potential prognostic biomarker
- for colorectal cancer. Oncol. Lett. 19, 4077–4087. https://doi.org/10.3892/ol.2020.11532 (2020).

 13. Qian, Y., Li, Y., Ge, Y., Song, W. & Fan, H. Elevated LncRNA TRERNA1 correlated with activation of HIF-1alpha predicts poor
- prognosis in hepatocellular carcinoma. *Pathol. Res. Pract.* **227**, 153612. https://doi.org/10.1016/j.prp.2021.153612 (2021).

 14. Luo, D. B. et al. LncRNA TRERNA1 promotes malignant progression of NSCLC through targeting FOXL1. *Eur. Rev. Med.* Pharmacol. Sci. 24, 1233-1242. https://doi.org/10.26355/eurrev_202002_20176 (2020).
- 15. Song, W. et al. ALKBH5-mediated N(6)-methyladenosine modification of TRERNA1 promotes DLBCL proliferation via p21 downregulation. Cell. Death Discov. 8, 25. https://doi.org/10.1038/s41420-022-00819-7 (2022)
- 16. Chen, Z. et al. Up-regulated LINC01234 promotes non-small-cell lung cancer cell metastasis by activating VAV3 and repressing BTG2 expression. J. Hematol. Oncol. 13, 7. https://doi.org/10.1186/s13045-019-0842-2 (2020).
- 17. Feng, Y. et al. Homeobox genes in cancers: from carcinogenesis to recent therapeutic intervention. Front. Oncol. 11, 770428. https://doi.org/10.3389/fonc.2021.770428 (2021).
- 18. Shao, L. et al. Effects of MLL5 and HOXA regulated by NRP1 on radioresistance in A549. Oncol. Lett. 21, 403. https://doi.org/10.3 892/ol.2021.12664 (2021).
- 19. Wang, W. et al. Down-regulated long non-coding RNA LHFPL3 antisense RNA 1 inhibits the radiotherapy resistance of nasopharyngeal carcinoma via modulating microRNA-143-5p/homeobox A6 axis. Bioengineered 13, 5421–5433. https://doi.org/1 0.1080/21655979.2021.2024386 (2022).
- 20. Guide for the Care and Use of Laboratory Animals. 8th ed. Washington (DC), (2011).
- 21. Livak, K. J. & Schmittgen, T. D. Analysis of relative gene expression data using real-time quantitative PCR and the 2(-Delta Delta
- C(T)) method. *Methods* 25, 402–408. https://doi.org/10.1006/meth.2001.1262 (2001).

 22. Ren, S. et al. N6-methyladenine- induced LINC00667 promoted breast cancer progression through m6A/KIAA1429 positive feedback loop. Bioengineered 13, 13462-13473. https://doi.org/10.1080/21655979.2022.2077893 (2022)
- Zhang, H. et al. PLK1 and HOTAIR accelerate proteasomal degradation of SUZ12 and ZNF198 during hepatitis B Virus-Induced liver carcinogenesis. Cancer Res. 75, 2363-2374. https://doi.org/10.1158/0008-5472.CAN-14-2928 (2015).
- 24. Alexander, M., Kim, S. Y. & Cheng, H. Update 2020: management of Non-Small cell lung Cancer. *Lung* **198**, 897–907. https://doi. org/10.1007/s00408-020-00407-5 (2020).
- 25. Wu, L., Zhou, Y. & Fu, J. KIAA1429 promotes nasopharyngeal carcinoma progression by mediating m6A modification of PTGS2. Crit. Rev. Immunol. 43, 15-27. https://doi.org/10.1615/CritRevImmunol.2023050249 (2023).
- 26. Li, N. et al. KIAA1429/VIRMA promotes breast cancer progression by m(6) A-dependent cytosolic HAS2 stabilization. EMBO Rep. 24, e55506. https://doi.org/10.15252/embr.202255506 (2023)
- 27. Xu, D., Wang, Z. & Li, F. KIAA1429 induces m6A modification of LINC01106 to enhance the malignancy of lung adenocarcinoma cells via the JAK/STAT3 pathway. Crit. Rev. Immunol. 44, 49-61. https://doi.org/10.1615/CritRevImmunol.2024052728 (2024).
- Zhong, M., Fang, Z., Guo, W. & Yu, X. Translation regulatory long non-coding RNA 1 negatively regulates cell radiosensitivity via the miR-22-3p/SP1 axis in non-small cell lung cancer. Clin. Respir J. 18, e13734. https://doi.org/10.1111/crj.13734 (2024).
- 29. Jia, D. et al. LINC02678 as a novel prognostic marker promotes aggressive Non-small-cell lung Cancer. Front. Cell. Dev. Biol. 9, 686975. https://doi.org/10.3389/fcell.2021.686975 (2021).
- 30. Hur, H., Lee, J. Y., Yun, H. J., Park, B. W. & Kim, M. H. Analysis of HOX gene expression patterns in human breast cancer. Mol. Biotechnol. 56, 64-71. https://doi.org/10.1007/s12033-013-9682-4 (2014).
- 31. Wu, F., Wu, S., Tong, H., He, W. & Gou, X. HOXA6 inhibits cell proliferation and induces apoptosis by suppressing the PI3K/Akt signaling pathway in clear cell renal cell carcinoma. Int. J. Oncol. 54, 2095-2105. https://doi.org/10.3892/ijo.2019.4789 (2019).

Author contributions

Y.L. and S.T. designed the experiments. S.T. drafted the manuscript. B.Y. prepared the figures and evaluated the results. Y.L. performed the statistical analysis of the data. All authors read and approved the final manuscript. None of the authors have any competing interests.

Funding

No funding received.

Declarations

Competing interests

The authors declare no competing interests.

Correspondence and requests for materials should be addressed to Y.L.

Additional information

Correspondence and requests for materials should be addressed to Y.L. or B.Y.

Reprints and permissions information is available at www.nature.com/reprints.

Publisher's note Springer Nature remains neutral with regard to jurisdictional claims in published maps and institutional affiliations.

Open Access This article is licensed under a Creative Commons Attribution-NonCommercial-NoDerivatives 4.0 International License, which permits any non-commercial use, sharing, distribution and reproduction in any medium or format, as long as you give appropriate credit to the original author(s) and the source, provide a link to the Creative Commons licence, and indicate if you modified the licensed material. You do not have permission under this licence to share adapted material derived from this article or parts of it. The images or other third party material in this article are included in the article's Creative Commons licence, unless indicated otherwise in a credit line to the material. If material is not included in the article's Creative Commons licence and your intended use is not permitted by statutory regulation or exceeds the permitted use, you will need to obtain permission directly from the copyright holder. To view a copy of this licence, visit http://creativecommons.org/licenses/by-nc-nd/4.0/.

© The Author(s) 2025